Research Square

Preprints are preliminary reports that have not undergone peer review.
They should not be considered conclusive, used to inform clinical practice,
or referenced by the media as validated information.

Estimation of methane emissions using TROPOMI and divergence analysis: A top-down assessment of Ghana's national-scale methane budget

Nadine Osei-Essah

nadine.oseiessah.u3@elms.hokudai.ac.jp

Hokkaido University

Yuichi S. Hayakawa

Hokkaido University

Research Article

Keywords: Methane Flux, TROPOMI, Emission Inventories, Ghana, Divergence Method

Posted Date: August 19th, 2026

DOI: https://doi.org/10.21203/rs.3.rs-8955196/v1

License: This work is licensed under a Creative Commons Attribution 4.0 International License.
Read Full License

Additional Declarations: No competing interests reported.

Estimation of methane emissions using TROPOMI and divergence analysis: A top-down assessment of Ghana's national-scale methane budget.

Nadine Osei-Essah[a] and Yuichi S. Hayakawa[b]

[a]Division of Environmental Science Development, Graduate School of Environmental Science, Hokkaido University, Sapporo. Japan. (nadine.oseiessah.u3@elms.hokudai.ac.jp; 0009-0000-7004-7136)

[b]Faculty of Environmental Earth Science, Hokkaido University. Sapporo. Japan. (hayakawa@eis.hokudai.ac.jp; 0000-0003-2053-8986)

Correspondence to nadine.oseiessah.u3@elms.hokudai.ac.jp

ABSTRACT
Methane (CH_4) emissions play an increasingly significant role in the climate impact of developing countries. Especially in Sub-Saharan Africa, where rapid population growth, expanding agricultural activities, and intensifying land-use change are altering emission patterns. These translate to severe implications for climate change, yet large uncertainties remain in the spatial distribution and emission sources in this region. We quantify methane emissions in Ghana using column-averaged methane observations from the Sentinel-5P TROPOspheric Monitoring Instrument (TROPOMI) combined with a divergence-based analysis. The observations were gridded, incorporated with wind vectors, and analyzed to characterize background concentrations and identify spatial patterns indicative of emission sources.

Multi-year atmospheric methane concentrations, surface and background levels, defined using the 10th percentile of observations, reveal relatively high concentrations in the southern part of the country. Methane fluxes exhibited strong directional asymmetry, with wind components indicating predominantly westward and southward transport. We inferred emissions, with most areas below 35 kg/km^2/h, attributable to emissions consistent with agricultural sources and mixed anthropogenic activities. The results reveal few but distinct methane emission hotspots with clear spatial structure over areas, highlighting contributions from both biogenic and anthropogenic sources. Validating the satellite-derived estimates with the Emissions Database for Global Atmospheric Research (EDGAR) showed an underestimation of the inventory. This approach demonstrates the capability of satellite-based methane observations, coupled with divergence analysis and inventory-based comparison, to support large-scale monitoring and assessment of methane emissions in data-scarce regions, providing a framework for improving constraints on regional methane budgets.

Keywords: Methane Flux, TROPOMI, Emission Inventories, Ghana, Divergence Method

INTRODUCTION

Greenhouse gas monitoring and estimation, of which methane forms a significant part of, have been riddled with a significant lack of long-term continuous effort (Franz et al. 2018), especially over Africa. Access to monitoring and mitigation technologies is limited (Igwe, 2025), despite Africa holding approximately 24% of the world's agricultural land (Ministry of Defence, UK, 2018), which is known to be a significant contributor to greenhouse gas emissions. Methane monitoring, especially on the African continent, is highly essential to mitigating emissions and fulfilling the Paris Agreement (Lunt et al. 2019; Nisbet et al. 2020; Werku et al. 2025).

Surface methane monitoring and estimation are possible using two complementary methodological frameworks: the bottom-up and the top-down approaches (Paul et al. 2024). The bottom-up inventories, such as EDGAR (global), rely heavily on emission factors and activity data across individual sectors, such as energy use and industry output (Crippa et al. 2018; Solazzo et al. 2021; Guizzardi et al. 2025), to estimate emissions, usually for point or sectoral sources. In contrast, top-down approaches infer emissions from atmospheric observation data, using atmospheric CH_4 concentrations and transfer models to estimate emissions at regional and global scales. Both methods have limitations (Zhao et al. 2023; Li et al. 2025); however, the top-down approach of using satellite observation data is increasingly preferred because it provides a more comprehensive estimate of total emissions (Tenkanen et al. 2025; Li et al. 2025). This is compared with the bottom-up approach, which can underestimate emissions due to incomplete data, inaccurate emission factors, and the challenge of handling a large number of individual measurements (National Academies of Sciences 2018; Tenkanen et al. 2025; Ioannidis et al. 2026).

Satellite observations, however, measure atmospheric concentrations rather than direct surface emissions, hence require analytical methods to infer concentrations into actual emission estimates. Over the years, several methodologies of methane flux estimation from satellite observation data have emerged, broadly classified into the mass-balance approach, divergence-based methods, atmospheric inversions, and plume-scale analysis, each with its distinct strengths and limitations in spatial resolution, computational cost, and data requirements (National Academies of Sciences 2018; Khiabani et al. 2024). Among these, the divergence method for flux estimation offers a computationally efficient alternative for estimating methane emissions, as it establishes a direct link between divergence and emissions given the long life span of CH4, making sinks negligible (Liu et al. 2021). It allows for the direct conversion of spatial gradients of atmospheric CH_4 into emission fluxes without the need for a priori information, atmospheric dispersion, and detailed transport or chemistry models like other frameworks (Huang et al. 2025b), but heavily relies on observational data and basic fluid dynamics (Huang et al. 2025a). This

method has been proven successful in various studies, such as (Liu et al. 2021, 2024; Li et al. 2023; Roberts et al. 2023; Gao and Xing 2025) in other parts of the world, and its application to the sub-Saharan context remains prominent. CH_4 emissions are heavily influenced by wind transport and other atmospheric processes (García et al. 2016); hence, measured values over a region do not always indicate a source of emission. Hence, the need to explore the use of the divergence method of flux estimation in the complex tropical meteorological conditions of Sub-Saharan Africa, which is characterised by the Intertropical Convergence Zone (ITCZ).

Africa's emerging economy makes it a prime area for GHG monitoring; however, monitoring and inventory development in most African countries are limited (Schneising et al. 2011) by sparse in-situ observations and an over-reliance on simplified bottom-up methodologies, such as the Tier 1 IPCC methodologies, to infer emissions rather than on the country-specific measurements offered by the top-down approach. While previous nation-wide studies (Chen et al., 2022, 2023; Hancock et al., 2025; Li et al., 2023; Shen et al., 2022) focused on high-emitting countries like the Americas, China, and the Middle East, sub-Saharan Africa has received limited attention despite being a significant contributor to global methane budget increases (Lunt et al., 2019; Pendergrass et al., 2025), attributable to wetland emissions. The select few satellite-based methane studies over Africa primarily focused on continental scale, specific point sources (wetlands, livestock) and multi-country inversions aggregating sub-Saharan African nations without country-specific attribution. Various studies have emerged using satellite data in GHG research around Africa, with a focus few on methane, such as (Lunt et al., 2019), who focused on wetland methane emissions, (Shikwambana et al. 2022; Sibiya et al. 2024; Masocha and Mhangara 2025) focusing on methane trends and variations, and (van Hove et al. 2025) on inferring emissions from livestock using a combination of remote sensing methods. In view of this and the limited ground-based measurements, there is therefore a need for expanded satellite-based methane studies across Africa to improve the accuracy and spatial representation of regional methane emission inventories.

The application of the flux divergence method over tropical Africa represents a significant methodological advancement and has proven effective for quantifying emissions from diverse sources, as is the case for Ghana.

This study, therefore, seeks to contribute to the growing knowledge of research on Sub-Saharan Africa by providing a the first comprehensive satellite-based national-scale quantification of methane in the sub-region for Ghana, detailing the total methane flux landscape by using a top-down approach and a simple divergence method of flux estimation. The specific objectives of the study are therefore to:

1. Apply a wind-based flux divergence method to TROPOMI XCH_4 data to isolate local emissions.

2. Generate a high-resolution regional flux density map for the entire country.

3. To compare these satellite-derived fluxes with an existing bottom-up inventory (EDGAR) to identify inventory discrepancies.

MATERIALS AND METHODS

STUDY AREA

The Republic of Ghana is in West Africa (4.5˚ N to 11.5˚ N), bounded on the west by Côte d'Ivoire, on the east by Togo, on the north by Burkina Faso and on the south by the Gulf of Guinea. It has a tropical climate influenced by the monsoon winds of West Africa (Nkrumah 2014) and is characterised by changing temperatures masked by seasons and elevation. The climatic conditions are warm and comparatively dry along the south-eastern coast, hot and humid in the southwest, and hot and dry in the north, with a mean annual temperature of 28.2°C in the north and 27.3°C in the south (Rohrig et al. 2019). The north side of the country records a unimodal rainy season from May to September with a mean annual precipitation of 900 mm, while the south records a bimodal rainy season, a major one from April to July and the minor one from September to November (Asare-Nuamah and Botchway 2019; Rohrig et al. 2019; Ampim et al. 2021); World Bank 2024) with a yearly mean of 1,500 mm (Rohrig et al. 2019). According to (Ampim et al., 2021), most land use and land cover changes across the country between 1995 and 2019 have been influenced by urbanisation and agriculture (69.1%), with land cover generally classified into built-up, grassland, other vegetation, bare area, agriculture, forest, wetland and waterbody.

In Ghana, CH_4 contributes significantly to the total GHG emissions due to widespread biomass use and increasing agricultural activity. It is known to be the most dominant Short-lived climate pollutant with an annual growth rate of 4.1%, with sources majorly from agriculture (50.7%), waste (42.2%), and the energy sector (7%) (Environmental Protection Agency (EPA) 2022). However, greenhouse gas emission estimation in Ghana follows the 2006 Intergovernmental Panel on Climate Change's guidelines, which involves compiling activity data and applying emission factors specific to each source category. This bottom-up inventory-based approach relies heavily on data availability, with emission data collected from national agencies such as the Environmental Protection Agency (EPA) and the Ghana Statistical Service (GSS), as well as other sector-specific ministries. This inventory is neither continuous nor high-resolution and lacks spatial precision and observational validation (Scarpelli, 2021). It does not capture the heterogeneous nature of CH_4 emissions, leaving a critical gap in the country's actual emission flux magnitude. A gridded inventory of national emissions will provide significant value in better characterising emissions and in comparing and testing established inventories against the emission estimates.

Data Source and Analysis

The methodology workflow employed for this study is as seen in Fig. 1. Data used for this research are XCH_4 L2 data from the TROPOMI Sentinel 5P, ERA5 reanalysis wind data from the European Centre for Medium-Range Weather Forecasts (ECMWF), ground–based methane data from the Emissions Database for Global Atmospheric Research (EDGAR). All data accessed were limited to the geographical bounds of Ghana for the study period of 2019 to 2023, except for the EDGAR, of which only 2021 was employed for validation.

Computing Surface XCH_4

Surface XCH_4 data were computed from the TROPOMI Sentinel 5P total column-averaged dry air mole fraction data product. Methods for this procedure were fashioned according to the study by (Li et al. 2023). Firstly, the lowest layer of the total data column was obtained from the CH_4 a priori vertical profile data, and that of the dry air density column as well was extracted from the TROPOMI official supporting data. Data was filtered to include only pixels with optimal quality value (qa_value > 0.5) to ensure only data of the highest quality were used. Surface XCH_4 was then calculated using the method by (1).

$$XCH_4 = \frac{VCH4}{Vair} \qquad (1)$$

Where V_{CH4} is the bottom layer of the TROPOMI CH_4 profile data, and V_{air} is the dry air density.

Surface Methane Estimation

To estimate the surface CH_4 concentration, the flux divergence method was used (2). The divergence method uses the continuity /transport equation to relate concentration gradients and wind to surface fluxes of the gas in question.

$$E = \Delta ((V - B)\vec{\omega}) \qquad (2)$$

Where V is the divergence of the CH_4 column at the surface, and B is the divergence of the regional background.

To detect the local methane enhancement, the local background was computed for each grid cell using the 11 × 11 grid-cell moving window approach. With each window, the 10^{th} percentile of methane was computed, successfully excluding localized high values and providing a robust estimate of the regional background. The background represents the baseline methane levels of the area.

To compute the flux, the methane enhancement was calculated as the difference between the observed methane (V) and the background (B) (3).

$$\text{Excess } CH_4 = V - B \qquad (3)$$

Validation and Uncertainty Quantification

To validate the results obtained, the estimated results for 2021 were compared to those of the EDGAR CH_4 emissions inventory (Janssen et al., 1999; S. Li et al., 2023),for the same year. Root Mean Square Error, Mean Absolute Error and Within Error Envelope were calculated for the estimated values and the inventories to evaluate associated errors (Hodson, 2022; S. Li et al., 2023).

A comprehensive uncertainty analysis was also performed to quantify errors in the emission estimates arising from the data sources using Monte Carlo propagation(Albert 2020; Yang et al. 2024; Mourtaday et al. 2024) (N=1000 iterations). TROPOMI retrieval precision, ±12 ppb (Lorente et al., 2021), was reduced to ±1.55 ppb after temporal averaging following standard error propagation. ERA5 wind field uncertainty was ±1.5 ms^{-1}, planetary boundary layer height was ±250 m from 25% of the assumed height of 1000 m for tropical West Africa, neglecting seasonal variability. Background concentration uncertainty was set at ±5 ppb, reflecting the 10^{th} percentile estimation method's sensitivity to spatial heterogeneity (Li et al., 2023). Spatial gradient discretization error (±20%) accounted for numerical truncation in the finite-difference divergence calculation. For each Monte Carlo iteration, input fields (XCH4, U-wind, V-wind, background, PBL height) were perturbed by Gaussian-distributed random noise scaled to their respective uncertainties. The flux divergence calculation was repeated with perturbed inputs, and an additional multiplicative gradient uncertainty factor (1 ± 20%) was applied to the resulting emission field. Annual total emissions were computed for each iteration by integrating emissions over latitude-varying grid cell areas and summing across Ghana's boundaries. The median and 16^{th} to 84^{th} percentile range of the 1000-member ensemble defined the best estimate and 68% confidence interval, respectively.

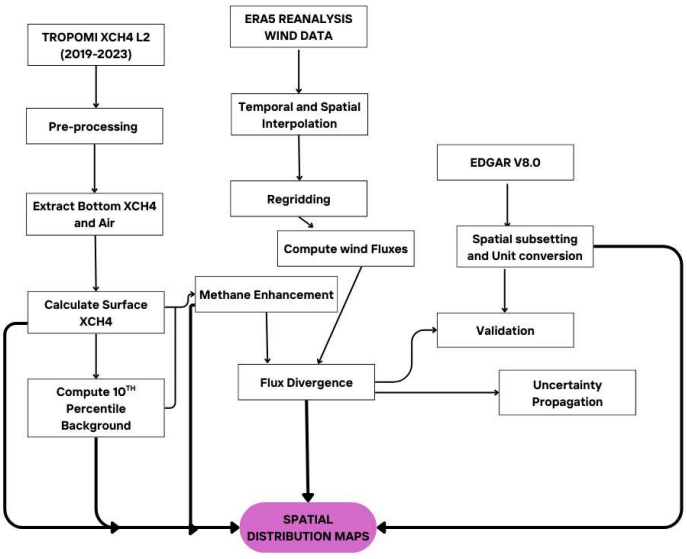


Fig. 1 Workflow chart illustrating the research methodology adopted in this study including data acqisition, preprocessing, analysis, and result evaluation.

Results

Spatial Distribution of CH_4 Concentrations

TROPOMI Sentinel-5P XCH_4 data from 2019 to 2023 was preprocessed and analyzed to create spatial distribution maps as shown in Fig. 2(a-d). The maps shown in Fig. 2 (a-d) depict the spatial distribution of atmospheric CH_4 column concentrations (Fig. 2a), surface-level (Fig. 2b), background-level concentrations (Fig. 2c), and the surface level enhancement (Fig. 2d) all of which showed significant variability across the country. Mean surface concentration was 1958 ± 1.55 ppb, with an enhancement mean of 3.1 ± 5.8 ppb above the local background mean, computed using an 11 × 11 grid-cell moving window approach. Atmospheric column concentrations exhibited spatial patterns with high values concentrated in the southern coastal part of the country and in areas within the Volta Basin, with an overall range of 1804 ppb to 1966 ppb reflecting elevated CH_4 concentrations.

The measured multi-year average surface level of CH_4 over the area mirrored that of the atmospheric column observations in terms of the spatial distribution pattern, with relatively higher concentrations in the south, along the coastal areas. The observed range was, however, slightly higher, 1914 ppb to 1990 ppb, than that of the atmospheric column range as shown in Fig. 2b, with a comparatively significantly high lower limit surpassing that of the atmospheric measurements by 110 ppb. Generally, there is a north-south gradient to all the visualized maps. The areas within the Volta River catchment showed significantly high concentrations in the background and surface concentration maps, whereas there was no or very little data observed from the atmospheric column distribution map.

National Inferred Emissions

The flux divergence method was used to estimate emissions based on the CH_4 enhancement (Fig 2d), computed from the surface-level and background-level concentrations (Figs. 2b and 2c). A combination of wind fluxes and the measured methane excess was employed in the simple divergence method. The zonal eastward and the meridional northward gradients both recorded negative values with ranges between -2.15 to -0.63 and -3.55 to -0.49, respectively, indicating westerly and southerly movement of wind consistent with West African monsoon circulation and dry season patterns. Positive fluxes indicate movement in the direction of the gradient, while negative values indicate movement opposite to the gradient. Plotting the wind data confirmed the results, with an annual average wind speed of within 2 m/s in the direction from the North-North-East to South-South-West. The observed wind fluxes were within the ranges of -61 ppb/m/s to 22 ppb/m/s for the Eastward flux and -147 ppb/m/s to 66 ppb/m/s for the northward flux. Visualization of the fluxes reveals the majority of the generated fluxes within the negative and very low positive values of the ranges, indicating general movement of the fluxes in the observed wind direction.

The estimated divergence flux emissions were within the ranges of less than 0 to greater than 87.6 kg/km^2/h. Only areas that recorded values higher than 0 (sources) were visualized on the divergence flux map (Figure 3). The southern coastal areas revealed relatively higher emissions compared to the northern part. Low to medium fluxes ranging between 9.8 and 35.7 kg/km^2/h were observed for most parts of the country. Fluxes along the coast were generally around 35.7 kg/km^2/h, with few areas exhibiting elevated fluxes (around 87.6 kg/km^2/h) observed primarily in the Greater Accra, Western region and within the Volta Region.

Ghana's total annual emissions were estimated to be 117 ± 41.0 CH_4 yr^{-1}.

Validation and Emission Uncertainty Budget

To evaluate the accuracy of the results, a density-based validation plot and spatial distribution maps were created to compare annual 2021 flux estimates of both the TROPOMI-inferred emissions and those of the EDGAR anthropogenic inventory. The plot (Fig 4) visualized the frequency distribution of paired emission estimates, allowing assessment of agreement patterns. Statistical analysis revealed a relatively high RMSE of 3.31, an MAE of 1.10, a relatively high WEE of 82.65%, and a negative Bias of 0.27.

The Monte Carlo uncertainty propagation (1000 iterations) yielded a best estimate of 109 ±38.4 Gg CH4 yr-1 (±35.2%, 68% confidence level), with samples ranging from 76.3 to 153.0 Gg CH_4 yr-1 (16th-84th percentiles).

Wind field uncertainty dominated the error budget (~45% of the total discrepancy), as Ghana's low wind speeds (mean 1.34 ms^{-1}) amplified the relative impact of the assumed ERA5's ±1.5ms^{-1} absolute uncertainty. Background concentration estimation contributed ~25% of the variance, reflecting the challenge of defining regional baselines in heterogeneous source regions using the 10th percentile method. Planetary boundary layer height assumptions (~15% of the variance), TROPOMI retrieval precision, and spatial gradient discretization errors (~5%) played secondary roles.

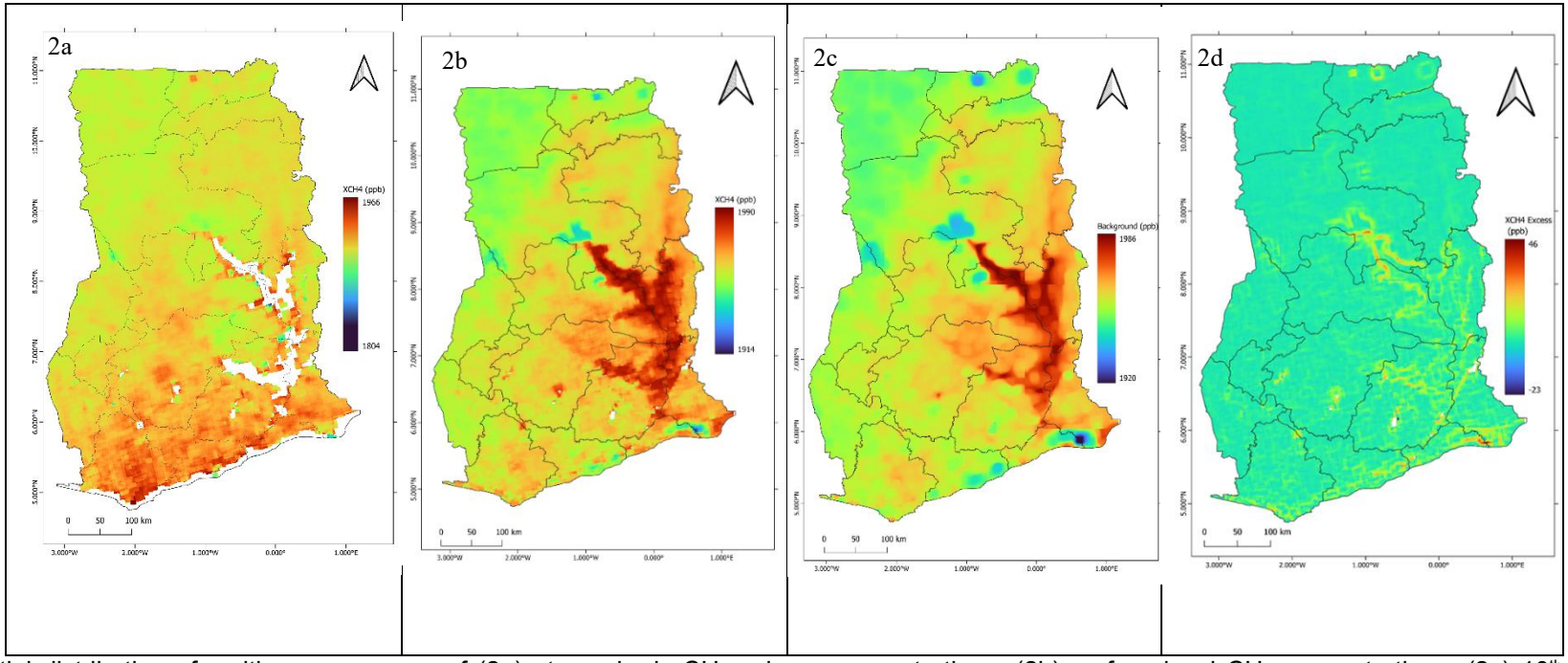


Fig 2: Spatial distribution of multi-year averages of (2a) atmospheric CH_4 column concentrations, (2b) surface-level CH_4 concentrations, (2c) 10^{th} percentile background CH_4 concentrations, and (2d) Enhancement/ excess CH_4 concentrations derived/or computed from TROPOMI observations for the period of 2019 to 2023. Legend represents the intensity of observations with warmer colors correlating to higher concentrations.

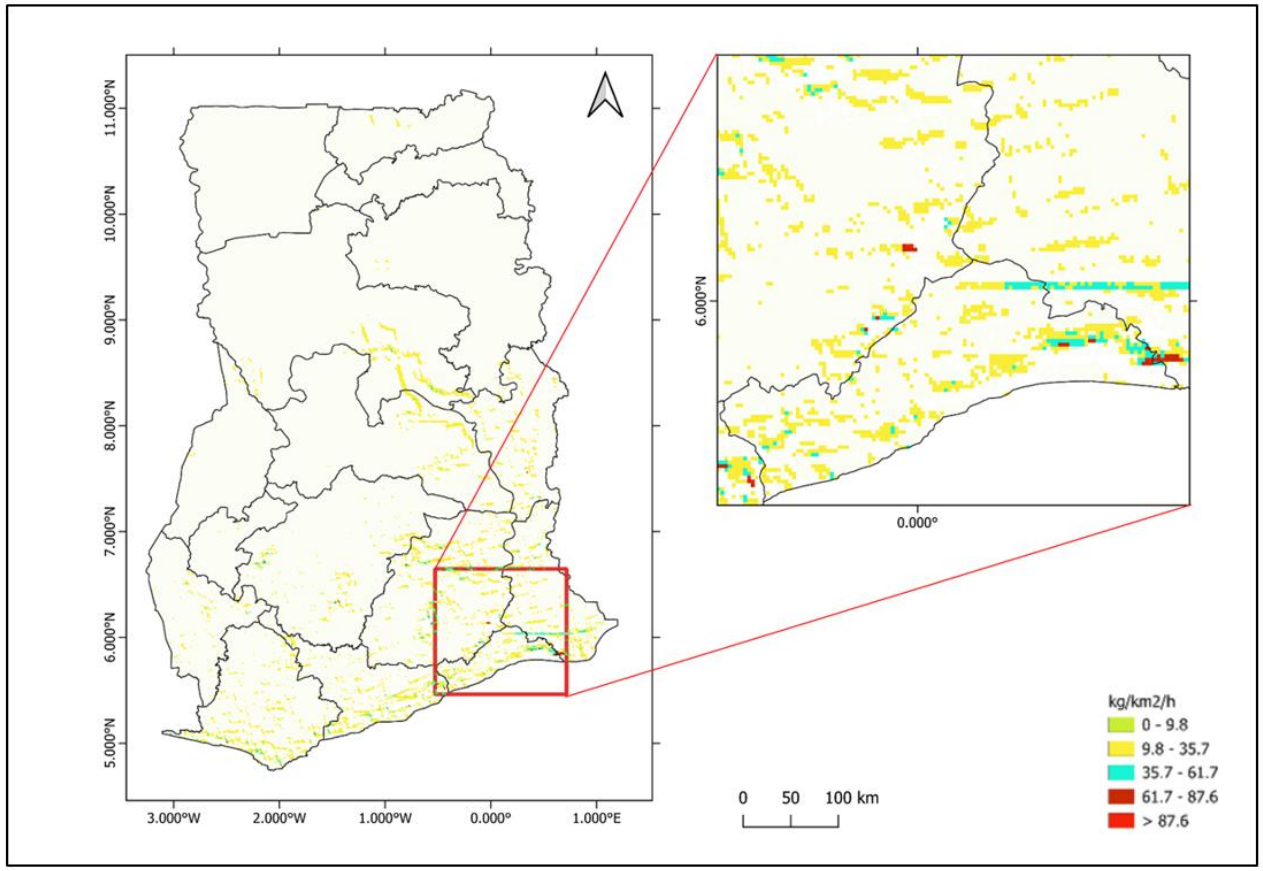


Fig 3: Spatial distribution and magnitudes of TROPOMI-inferred methane emissions from divergence analysis across Ghana. Legend represents emission intensity with warmer colors indicating higher levels.

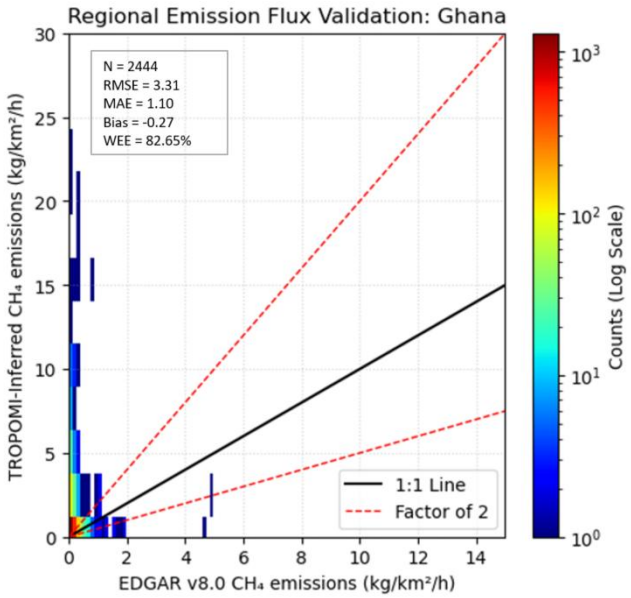


Fig 4: Bivariate density comparison between EDGAR v8.0 methane emission fluxes and TROPOMI-divergence inferred emission fluxes over Ghana with associated errors. Colors indicate the density of the grid-cell pairs, with 1: 1 line and a factor-of-two agreement bounds.

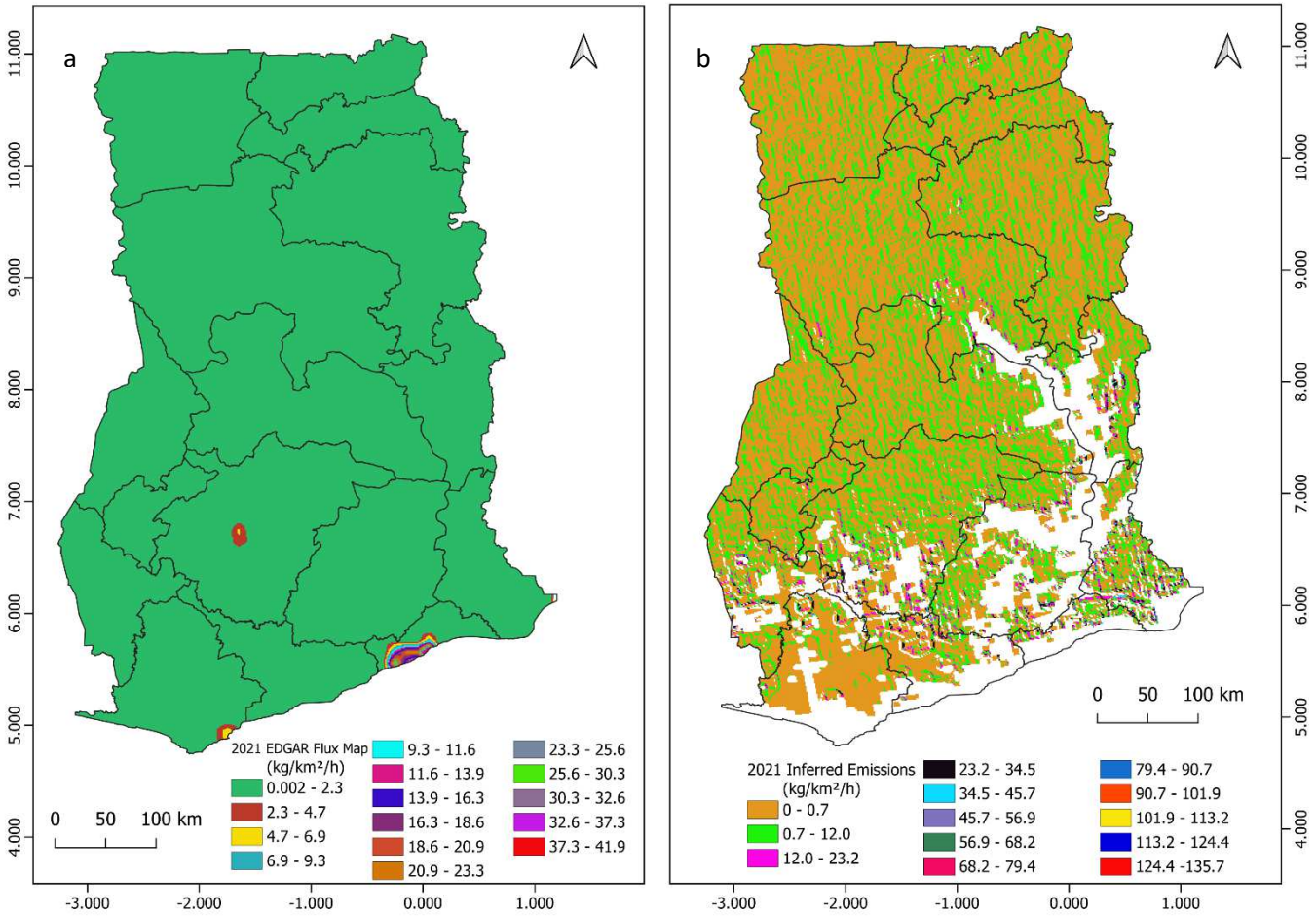

a
b
11.000
10.000
9.000
8.000
7.000
6.000
5.000
4.000
-3.000
-2.000
-1.000
0.000
1.000
0 50 100 km
2021 EDGAR Flux Map
(kg/km²/h)
0.002 - 2.3
2.3 - 4.7
4.7 - 6.9
6.9 - 9.3
9.3 - 11.6
11.6 - 13.9
13.9 - 16.3
16.3 - 18.6
18.6 - 20.9
20.9 - 23.3
23.3 - 25.6
25.6 - 30.3
30.3 - 32.6
32.6 - 37.3
37.3 - 41.9
2021 Inferred Emissions
(kg/km²/h)
0 - 0.7
0.7 - 12.0
12.0 - 23.2
23.2 - 34.5
34.5 - 45.7
45.7 - 56.9
56.9 - 68.2
68.2 - 79.4
79.4 - 90.7
90.7 - 101.9
101.9 - 113.2
113.2 - 124.4
124.4 -135.7

Fig 5: Spatial comparison of EDGAR inventory emissions and TROPOMI-divergence inferred emissions for 2021 across Ghana. (a.) EDGAR v8.0 methane emissions flux spatial distribution map and (b.) TROPOMI-inferred methane emissions flux spatial distribution map. Legends indicate intensity of emissions ranging from lowest to highest (units: $kg/km^2/h$).

Discussion

Spatial Distribution of Methane

The average methane concentrations across the country from 2019 to 2022 showed significant spatial variability. Relatively higher concentrations were clustered in the southern part of the country, which have a high density and diversity of anthropogenic activities such as urbanization, agriculture, mining, etc., and water bodies and wetlands, as compared to the northern part of the country. The majority of the highest concentrations were observed along the coastal areas. The overall range of 1804 ppb to 1966 ppb observed reflects elevated CH_4 concentrations, which are, however, consistent with the global averages reported by Lan et al. (2022).

The higher concentration range of multi-year average surface level of CH_4 over the area relative to the atmospheric column observations is consistent with literature as reported by Schneising et al., (2011), in their study of long-term methane analysis. They noted that surface methane concentrations are always higher than column concentrations, a phenomenon attributable to the relative closeness of these surface concentrations to the earth's surface, where concentrations are strongly influenced by emission sources and sinks. Also, concentrations within the atmospheric column are integrated throughout the entire column, thereby creating a smoothening effect which eliminates concentration spikes (Veefkind et al. 2012; Buchwitz et al. 2017; Lorente et al. 2021). However, both observations indicate relatively high concentrations in the southern parts of the country, compared to the northern parts. The observed concentrations and spatial variability can, be as a result of the culmination of CH_4 accumulation and transport, given that it has a long atmospheric lifespan (Oh et al., 2025; Saunois et al., 2025; Zhang et al., 2023). This is confirmed by the observations from the calculated background concentrations using the 10^{th} percentile approach, depicting a similar high range of concentrations.

The high concentrations observed in all the spatial maps over the visible wetland areas, notably along the banks of the Volta River within the Volta River catchment is consistent with literature with evidence from Kim et al. (2016) who report observing relatively higher CH_4 emissions from river deltas in their study of GHG emissions from natural ecosystems and agricultural lands. Consecutively, the higher concentrations within the wetland areas, primarily located within the southern part of the country where most of the higher emissions are observed, could be contributed to by transported emissions from the movement of wind fluxes in the south-west direction as observed in this study. The observed negative fluxes indicate a weak movement opposite to the gradients; the east gradient suggested a dominant westward direction, while the north gradient indicated a net southward movement of emissions.

The few spots in the northern part of the country that recorded relatively high concentrations could possibly be attributed to agriculture (Arthur and Baidoo 2011; Environmental Protection Agency (EPA) 2022; Abdulai et al. 2023).

Methane Quantification Using Divergence

In quantifying methane emissions in the study area, a combination of wind fluxes (online resource 3) and the measured methane enhancement was used in a simple divergence method. The estimation was performed on temporarily averaged data to reduce noise and provide a more stable emission estimate consistent with previous divergence-based studies (Li et al., 2023; Liu et al., 2021). The observed fluxes' direction opposite to the wind gradients indicates CH_4 enhancements are actively distributed by winds and transport and are directionally dependent. Spatial patterns may therefore be shaped by regional circulation and not just local emissions. The easterly flow transports methane-enriched air westward from emission sources, while the weak northerly winds carry emissions southward all driving emissions in the general south-western direction and possibly influenced by the North Eastern trade winds.

Most of the divergence estimates are low, with the majority of the areas recording concentrations below 35.7 $kg/km^2/hr$. These relatively moderate emission intensities indicate sources related to agriculture, such as rice cultivation, livestock density, and small-scale anthropogenic activities, as opposed to super emitters such as fossil fuel infrastructure or large landfills, (Crippa et al. 2024; Zolani Ndlovu 2024), reinforcing the agricultural (Environmental Protection Agency (EPA) 2022) and mixed source nature of emissions.

Validation of TROPOMI-inferred emissions

The statistical results depict a notable divergence between the inferred fluxes and the EDGAR inventory. The inferred fluxes have a much wider magnitude range and very limited pixel-level agreement with the EDGAR inventory. This limited agreement was particularly heightened at lower emission magnitudes of the EDGAR inventory where a dominant and frequent overestimation pattern was observed, especially where EDGAR emissions are close to zero. This phenomenon was also noted by Xingyu Li et al. (2025). All the statistical evidences indicates the presence of localized discrepancies and an error in characterizing high-intensity areas rather than the diffuse emissions. This is evident from the density plot, where the EDGAR distribution shows very few areas with high concentrations as compared to the inferred emissions, an observation also noted by Xiaofan Li et al. (2025), especially in urban areas. This is possibly attributable to inaccurate emission factor data and also to the exclusion of biogenic and natural sources of emissions. Also, the high-weighted error estimate emphasizes the large deviation between the estimated values and the EDGAR values, while the moderate RMSE, reflected

likely methodological differences between the two approaches rather than an error on the part of the inferred emissions. The inferred estimation captured diffuse and variable source concentrations that may not be fully represented in the inventory, particularly in tropical environments that exhibit greater dispersion likely influenced by convective mixing, diffuse biogenic sources, and higher temporal emissions. This is accentuated by East et al., (2025), who in their study noted sub-Saharan Africa to be a major contributor to the underreported global livestock emissions, with a methane intensity 7 times higher than in North America or East Asia.

Notably, the distribution maps (Fig 5) visualizes the divergence between the two datasets observed from the statistical analysis. The TROPOMI-inferred dataset shows a peak fluxes reaching about 136 kg/km^2/h, primarily concentrated in the southernmost part of the country, compared to a relatively low EDGAR peak most flux of 41.9 kg/km^2/hr located right along the coast of Greater Accra. Hotspots locations of both datasets were consistent in the south, over areas close to the coastal areas in the Greater Accra and Volta Regions of the country. The concentration ranges of the two datasets, however, show a gross underestimation of the EDGAR inventories, as has been reported by several other studies, such as Crippa et al., (2018), Li et al., (2023), Maasakkers et al., (2019), and Worden et al., 2023). The inferred flux concentrations across most of the country were higher in concentration than those of EDGAR. The spatial distribution of the inferred emissions, however, had lower spatial density as compared to the EDGAR inventory. All areas along the coast and over the distinct wetland regions in the Volta River Catchment were data-sparse. This observation could be attributed to certain factors (cloud interference or aerosol loading) that could be attenuating the satellite signal over these highly possible source regions, Figure 5(b).

While the spatial distribution of the inferred emissions shows relative consistency with EDGAR in terms of some hotspot locations, the overall spatial coverage of the inferred emissions was lower than that of the inventory. The density-based validation, therefore, reveals a systematic overestimation in magnitude and an underestimation of data coverage across the country in terms of the inferred emissions.

Uncertainty Analysis and Methodological Limitations

A significant limitation of this study is the spatial coverage of valid TROPOMI retrievals over Ghana. Persistent cloud cover and elevated aerosol loading lead to sparser emission estimates in the cloud-prone southern regions (Dubey et al. 2023; Mehrdad and Du 2025; Clow et al. 2025), where emissions may be highest. Cloud-driven sampling bias, resulting persistent lack of data over potential coastal emission hotspots (particularly Greater Accra, Western Region, and Volta Region) introduces systematic spatial undersampling that remains unquantified. If these areas emit at twice the observed mean, missing emissions could significantly increase annual totals.

The dominant wind field uncertainty, similar to studies by Nassar et al. (2022) and Varon et al., (2018) at 40% and 30% respectively, suggests targeted improvements. As noted by Li et al. (2023), there are significant errors associated with wind speeds and directions, making wind field accuracy a primary limitation in divergence flux calculations.

Our ±35% uncertainty, while consistent with flux divergence literature (Gao & Xing, 2025: ±45%), likely underestimates true errors due to several unquantified sources. Uncertainties such as regional biases in TROPOMI XCH_4, especially in low-albedo regions (estimated at 6.7 ppbv), cross-boundary transport uncertainty (Locatelli et al. 2013), were not propagated through the Monte Carlo framework; a hypothetical 5 ppb positive bias would inflate our estimate by ~60 Gg yr-1 (55%), potentially explaining part of the EDGAR discrepancy.

Future studies could employ resolutions to address these uncertainties such as; Targeted surface wind monitoring network stations to reduce wind-driven errors, lowering total uncertainty to ±25-30%. Alternative background estimation methods could also halve background-driven uncertainty. Systematic biases-particularly TROPOMI calibration, cloud sampling, and boundary transport should be prioritized for future studies through aircraft validation campaigns and high-resolution regional inversions.

Conclusion

This study presents the first national-scale, satellite-based quantification of surface-level CH_4 emissions for Ghana using a flux divergence approach applied to Sentinel-5P TROPOMI observations. By adapting this methodology to the climatic conditions of tropical Africa, we demonstrate the applicability of satellite emission mapping in data-sparse sub-Saharan African nations.

Annual mean methane fluxes over Ghana were found to be of low to moderate levels, exhibiting spatial patterns consistent with both natural and anthropogenic sources with relatively view hotspot areas. The inferred emission estimates reveal high concentrations in the southern part of Ghana (particularly in the Greater Accra, Western, and Volta Regions) and low concentrations in the northern part of the country. This north-south gradient observed aligns with population density, agricultural activity, and wetland distribution across the country.

The inferred emissions were compared with the EDGAR v8.0 inventory to evaluate consistency in both spatial distribution and emission magnitude. Our study observed an underestimation of emissions in the EDGAR inventories, and a spatial coverage limitation of the inferred dataset was also observed, which could be attributed to climatic conditions attenuating satellite observations.

The findings of this study demonstrate the value of satellite-derived emissions in successfully capturing dominant spatial patterns of methane emissions across Ghana, with its diverse emission source profile. By demonstrating its applicability, this study establishes a replicable framework for systematic national methane monitoring across sub-Saharan Africa, with similar meteorological regimes and where ground-based monitoring systems are limited. This study also supports Ghana's commitment under the Global Methane Pledge and the Paris Agreement as the region experiences rapid economic development and GHG monitoring becomes increasingly critical for ensuring accountability in global climate mitigation efforts.

Overall, the findings confirm that satellite-derived flux divergence methods are a viable tool for methane emission monitoring in Sub-Saharan Africa and provide a foundation for enhanced greenhouse gas assessments in data-limited regions.

Statements and Declarations

The authors declare no competing interests relevant to the content of this article.

This research received no funds, grants, or other support from any funding agency for conducting this study.

Data Availability

SentineL-5P TROPOMI data are freely available from the Copernicus Data Space Ecosystem (https://dataspace.copernicus.eu/). ERA5 Reanalysis wind data are freely available from the Copernicus Climate Data Store (cds.climate.copernicus.eu/datasets/reanalysis-era5-single-levels?tab=download). The EDGAR v8.0 data are freely available at https://edgar.jrc.ec.europa.eu/. All other processed datasets generated during this study are available from the corresponding author upon request.

References

Abdulai IA, Dongzagla A, Ahmed A (2023) Urban livestock rearing and the paradox of sustainable cities and urban governance in West Africa: Empirical evidence from Wa, Ghana. Urban Governance 3:. https://doi.org/10.1016/j.ugj.2023.06.004

Albert DR (2020) Monte Carlo Uncertainty Propagation with the NIST Uncertainty Machine. J Chem Educ 97:1491–1494. https://doi.org/10.1021/acs.jchemed.0c00096

Ampim PAY, Ogbe M, Obeng E, et al (2021) Land cover changes in ghana over the past 24 years. Sustainability (Switzerland) 13:. https://doi.org/10.3390/su13094951

Arthur R, Baidoo MF (2011) Harnessing methane generated from livestock manure in Ghana, Nigeria, Mali and Burkina Faso. Biomass Bioenergy 35:. https://doi.org/10.1016/j.biombioe.2011.09.009

Asare-Nuamah P, Botchway E (2019) Understanding climate variability and change: analysis of temperature and rainfall across agroecological zones in Ghana. Heliyon 5:. https://doi.org/10.1016/j.heliyon.2019.e02654

Buchwitz M, Schneising O, Reuter M, et al (2017) Satellite-derived methane hotspot emission estimates using a fast data-driven method. Atmos Chem Phys 17:5751–5774. https://doi.org/10.5194/acp-17-5751-2017

Chen Z, Jacob DJ, Gautam R, et al (2023) Satellite quantification of methane emissions and oil–gas methane intensities from individual countries in the Middle East and North Africa: implications for climate action. Atmos Chem Phys 23:5945–5967. https://doi.org/10.5194/acp-23-5945-2023

Chen Z, Jacob DJ, Nesser H, et al (2022) Methane emissions from China: a high-resolution inversion of TROPOMI satellite observations. Atmos Chem Phys 22:10809–10826. https://doi.org/10.5194/acp-22-10809-2022

Clow GL, Lovenduski NS, Levy MN, et al (2025) Accounting for Satellite Sampling Bias in the Validation of CESM2 Sea Surface Temperature and Chlorophyll. J Adv Model Earth Syst 17:. https://doi.org/10.1029/2024MS004908

Crippa M, Guizzardi D, Muntean M, et al (2018) Gridded emissions of air pollutants for the period 1970–2012 within EDGAR v4.3.2. Earth Syst Sci Data 10:1987–2013. https://doi.org/10.5194/essd-10-1987-2018

Crippa M, Guizzardi D, Pagani F, et al (2024) Insights into the spatial distribution of global, national, and subnational greenhouse gas emissions in the Emissions Database for Global Atmospheric Research (EDGAR v8.0). Earth Syst Sci Data 16:2811–2830. https://doi.org/10.5194/essd-16-2811-2024

Dubey L, Cooper J, Staffell I, et al (2023) Comparing satellite methane measurements to inventory estimates: A Canadian case study. Atmos Environ X 17:100198. https://doi.org/10.1016/j.aeaoa.2022.100198

East JD, Jacob DJ, Jervis D, et al (2025) Worldwide inference of national methane emissions by inversion of satellite observations with UNFCCC prior estimates. Nat Commun 16:11004. https://doi.org/10.1038/s41467-025-67122-8

Environmental Protection Agency (EPA) G (2022) Ghana's Fifth National Greenhouse Gas Inventory 2021 National Greenhouse Gas Emissions Report

Franz D, Acosta M, Altimir N, et al (2018) Towards long-term standardised carbon and greenhouse gas observations for monitoring Europe's terrestrial ecosystems: a review. Int Agrophys 32:439–455. https://doi.org/10.1515/intag-2017-0039

Gao M, Xing Z (2025) Estimating Methane Emissions by Integrating Satellite Regional Emissions Mapping and Point-Source Observations: Case Study in the Permian Basin. Remote Sens (Basel) 17:3143. https://doi.org/10.3390/rs17183143

García MÁ, Sánchez ML, Pérez IA, et al (2016) Influence of atmospheric stability and transport on CH 4 concentrations in northern Spain. Science of The Total Environment 550:157–166. https://doi.org/10.1016/j.scitotenv.2016.01.099

Guizzardi D, Becker W, Pagani F, et al (2025) Global up-to date emissions using the EDGAR Fast-Track methodology. Sci Data 12:1243. https://doi.org/10.1038/s41597-025-04806-2

Hancock SE, Jacob DJ, Chen Z, et al (2025) Satellite quantification of methane emissions from South American countries: a high-resolution inversion of TROPOMI and GOSAT observations. Atmos Chem Phys 25:797–817. https://doi.org/10.5194/acp-25-797-2025

Hodson TO (2022) Root-mean-square error (RMSE) or mean absolute error (MAE): when to use them or not. Geosci Model Dev 15:5481–5487. https://doi.org/10.5194/gmd-15-5481-2022

Huang Y, Han G, Shi T, et al (2025a) FI-SCAPE: A Divergence Theorem Based Emission Quantification Model for Air/Spaceborne Imaging Spectrometer Derived X $_{CH4}$ Observations. IEEE J Sel Top Appl Earth Obs Remote Sens 18:255–272. https://doi.org/10.1109/JSTARS.2024.3490896

Huang Y, Han G, Yi J, et al (2025b) Rapid Methane Flux Estimation Combining MethaneSAT and Sentinel-5P Observations: A Case Study of Turkmenistan. Geophys Res Lett 52:. https://doi.org/10.1029/2025GL119369

Igwe E (2025) Assessing sub-Saharan Africa's GHG emissions from croplands: environmental impacts and sustainable mitigation strategies. Environ Monit Assess 197:208. https://doi.org/10.1007/s10661-025-13633-2

Ioannidis E, Meesters A, Steiner M, et al (2026) An inter-comparison of inverse models for estimating European CH $_4$ emissions. Earth Syst Sci Data 18:167–198. https://doi.org/10.5194/essd-18-167-2026

Janssen LHJM, Olivier JGJ, van Amstel AR (1999) Comparison of CH4 emission inventory data and emission estimates from atmospheric transport models and concentration measurements. Environ Sci Policy 2:295–314. https://doi.org/10.1016/S1462-9011(99)00020-9

Khiabani PM, Danala G, Jentner W, Ebert D (2024) Challenges in Data Integration, Monitoring, and Exploration of Methane Emissions: The Role of Data Analysis and Visualization. In: 2024 IEEE Workshop on Energy Data Visualization (EnergyVis). IEEE, pp 1–6

Kim D-G, Thomas AD, Pelster D, et al (2016) Greenhouse gas emissions from natural ecosystems and agricultural lands in sub-Saharan Africa: synthesis of available data and suggestions for further research. Biogeosciences 13:4789–4809. https://doi.org/10.5194/bg-13-4789-2016

Lan X, Thoning KW, Dlugokencky (2022) Trends in globally-averaged CH4, N2O, and SF6 determined from NOAA Global Monitoring Laboratory measurements

Li S, Wang C, Gao P, et al (2023) High-Spatial-Resolution Methane Emissions Calculation Using TROPOMI Data by a Divergence Method. Atmosphere (Basel) 14:388. https://doi.org/10.3390/atmos14020388

Liu M, van der A R, van Weele M, et al (2021) A New Divergence Method to Quantify Methane Emissions Using Observations of Sentinel-5P TROPOMI. Geophys Res Lett 48:. https://doi.org/10.1029/2021GL094151

Liu M, van der A R, van Weele M, et al (2024) Current potential of CH $_4$ emission estimates using TROPOMI in the Middle East. Atmos Meas Tech 17:5261–5277. https://doi.org/10.5194/amt-17-5261-2024

Li Xingyu, Cheng T, Zhu H, et al (2025) High-Resolution Satellite Reveals the Methane Emissions from China's Coal Mines. Remote Sens (Basel) 17:220. https://doi.org/10.3390/rs17020220

Li Xiaofen, Zhang Y, de Leeuw G, et al (2025) A Review of City-Scale Methane Flux Inversion Based on Top-Down Methods. Remote Sens (Basel) 17:3152. https://doi.org/10.3390/rs17183152

Locatelli R, Bousquet P, Chevallier F, et al (2013) Impact of transport model errors on the global and regional methane emissions estimated by inverse modelling. Atmos Chem Phys 13:9917–9937. https://doi.org/10.5194/acp-13-9917-2013

Lorente A, Borsdorff T, Butz A, et al (2021) Methane retrieved from TROPOMI: Improvement of the data product and validation of the first 2 years of measurements. Atmos Meas Tech 14:. https://doi.org/10.5194/amt-14-665-2021

Lunt MM, Palmer PP, Feng L, et al (2019) An increase in methane emissions from tropical Africa between 2010 and 2016 inferred from satellite data. Atmos Chem Phys 19:. https://doi.org/10.5194/acp-19-14721-2019

Maasakkers JD, Jacob DJ, Sulprizio MP, et al (2019) Global distribution of methane emissions, emission trends, and OH concentrations and trends inferred from an inversion of GOSAT satellite data for 2010–2015. Atmos Chem Phys 19:7859–7881. https://doi.org/10.5194/acp-19-7859-2019

Masocha BL, Mhangara P (2025) Satellite-driven assessment of methane trends, seasonal variability, and emission hotspots in Botswana's Central and Ngamiland Regions. Environ Monit Assess 197:

Mehrdad SM, Du K (2025) Satellite-Based Methane Emission Monitoring: A Review Across Industries. Remote Sens (Basel) 17:3674. https://doi.org/10.3390/rs17223674

Ministry of Defence, UK (2018) Global Strategic Trends: The Future Starts Today

Mourtaday N, Bati M, Blanco S, et al (2024) Monte Carlo simulation of atmospheric radiative forcings using a path-integral formulation approach for spectro-radiative sensitivities. J Quant Spectrosc Radiat Transf 327:109123. https://doi.org/10.1016/j.jqsrt.2024.109123

Nassar R, Moeini O, Mastrogiacomo J-P, et al (2022) Tracking CO2 emission reductions from space: A case study at Europe's largest fossil fuel power plant. Frontiers in Remote Sensing 3:. https://doi.org/10.3389/frsen.2022.1028240

National Academies of Sciences E and M (2018) Improving Characterization of Anthropogenic Methane Emissions in the United States. National Academies Press, Washington, D.C.

Nisbet EG, Fisher RE, Lowry D, et al (2020) Methane Mitigation: Methods to Reduce Emissions, on the Path to the Paris Agreement. Reviews of Geophysics 58:. https://doi.org/10.1029/2019RG000675

Nkrumah F (2014) DYNAMIC ANALYSIS OF THE WEST AFRICAN MONSOON AND ITS VARIABILITY OVER GHANA

Paul J, Faye L, Dia M, et al (2024) Exploring Methane Emissions in Africa Introduction

Pendergrass DC, Jacob DJ, Balasus N, et al (2025) Trends and seasonality of 2019–2023 global methane emissions inferred from a localized ensemble transform Kalman filter (CHEEREIO v1.3.1) applied to TROPOMI satellite observations. Atmos Chem Phys 25:14353–14369. https://doi.org/10.5194/acp-25-14353-2025

Roberts C, IJzermans R, Randell D, et al (2023) Avoiding methane emission rate underestimates when using the divergence method. Environmental Research Letters 18:114033. https://doi.org/10.1088/1748-9326/ad0252

Rohrig F, Lange S, Aschenbrenner P, et al (2019) Climate-risk-profile-Ghana

Saunois M, Martinez A, Poulter B, et al (2025) Global Methane Budget 2000–2020. Earth Syst Sci Data 17:1873–1958. https://doi.org/10.5194/essd-17-1873-2025

Schneising O, Buchwitz M, Reuter M, et al (2011) Long-term analysis of carbon dioxide and methane column-averaged mole fractions retrieved from SCIAMACHY. Atmos Chem Phys 11:2863–2880. https://doi.org/10.5194/acp-11-2863-2011

Shen L, Gautam R, Omara M, et al (2022) Satellite quantification of oil and natural gas methane emissions in the US and Canada including contributions from individual basins. Atmos Chem Phys 22:11203–11215. https://doi.org/10.5194/acp-22-11203-2022

Shikwambana L, Mokgoja B, Mhangara P (2022) A Qualitative Assessment of the Trends, Distribution and Sources of Methane in South Africa. Sustainability 14:3528. https://doi.org/10.3390/su14063528

Sibiya SS, Mhangara P, Shikwambana L (2024) Seasonal and trend variation of methane concentration over two provinces of South Africa using Sentinel-5p data. Environ Monit Assess 196:713. https://doi.org/10.1007/s10661-024-12871-0

Solazzo E, Crippa M, Guizzardi D, et al (2021) Uncertainties in the Emissions Database for Global Atmospheric Research (EDGAR) emission inventory of greenhouse gases. Atmos Chem Phys 21:5655–5683. https://doi.org/10.5194/acp-21-5655-2021

Tenkanen MK, Tsuruta A, Denier van der Gon H, et al (2025) Partitioning anthropogenic and natural methane emissions in Finland during 2000–2021 by combining bottom-up and top-down estimates. Atmos Chem Phys 25:2181–2206. https://doi.org/10.5194/acp-25-2181-2025

van Hove A, Aalstad K, Lind V, et al (2025) Inferring methane emissions from African livestock by fusing drone, tower, and satellite data. Biogeosciences 22:4163–4186. https://doi.org/10.5194/bg-22-4163-2025

Varon DJ, Jacob DJ, McKeever J, et al (2018) Quantifying methane point sources from fine-scale satellite observations of atmospheric methane plumes. Atmos Meas Tech 11:5673–5686. https://doi.org/10.5194/amt-11-5673-2018

Veefkind JP, Aben I, McMullan K, et al (2012) TROPOMI on the ESA Sentinel-5 Precursor: A GMES mission for global observations of the atmospheric composition for climate, air quality and ozone layer applications. Remote Sens Environ 120:. https://doi.org/10.1016/j.rse.2011.09.027

Werku BC, Bulto TW, Geleto TC (2025) Impact of methane emissions on greenhouse gas emissions in selected sub-Saharan African countries: a comprehensive analysis and policy framework for mitigation strategies. Environ Sci Eur 37:199. https://doi.org/10.1186/s12302-025-01214-6

Worden JR, Pandey S, Zhang Y, et al (2023) Verifying Methane Inventories and Trends With Atmospheric Methane Data. AGU Advances 4:. https://doi.org/10.1029/2023AV000871

Yang F, Forootan E, Liu S, Schumacher M (2024) A Monte Carlo Propagation of the Full Variance-Covariance of GRACE-Like Level-2 Data With Applications in Hydrological Data Assimilation and Sea-Level Budget Studies. Water Resour Res 60:. https://doi.org/10.1029/2023WR036764

Zhang S, Ma J, Zhang X, Guo C (2023) Atmospheric remote sensing for anthropogenic methane emissions: Applications and research opportunities. Science of the Total Environment 893

Zhao Y, Saunois M, Bousquet P, et al (2023) Reconciling the bottom-up and top-down estimates of the methane chemical sink using multiple observations. Atmos Chem Phys 23:789–807. https://doi.org/10.5194/acp-23-789-2023

Zolani Ndlovu (2024) Assessing the role of area sources in air quality: A comprehensive review. World Journal of Advanced Research and Reviews 23:1462–1472. https://doi.org/10.30574/wjarr.2024.23.2.2495

Supplementary Files

This is a list of supplementary files associated with this preprint. Click to download.

- SupplementaryInformation.docx